Computers and Concrete, Vol. 1, No. 3 (2004) 355-369
DOI: http://dx.doi.org/10.12989/cac.2004.1.3.355

Finite element modeling of slab-on-beam concrete bridge superstructures

Michael D. Patrick† and X. Sharon Huo‡

Department of Civil and Environmental Engineering, Tennessee Technological University, P.O. Box 5015, Cookeville, TN 38505, U.S.A.

Abstract. This paper presents a study of four finite element techniques that can be used to model slab-on-beam highway bridges. The feasibility and correctness of each modeling technique are examined by applying them to a prestressed concrete I-beam bridge and a prestressed concrete box-beam bridge. Other issues related to bridge modeling such as torsional constant, support conditions, and quality control check are studied in detail and discussed in the paper. It is found that, under truck loading, the bending stress distribution in a beam section depends on the modeling technique being utilized. It is observed that the behavior of the bridge superstructure can be better represented when accounting for composite behavior between the supporting beams and slab.

Keywords: bridges; finite element modeling; modeling techniques; beam offset; torsional constant; support conditions; diaphragm effect; live load distribution factor.

1. Introduction

Finite element analysis (FEA) has proven to be a useful tool for the structural analysis of buildings and highway bridge superstructures. Research has shown that different modeling techniques as well as different types of elements can be used when modeling a bridge superstructure (Mabsout, *et al.* 1997, Eom and Nowak 2001). Some research has also shown that, depending on the bridge type and geometry, some modeling techniques may yield more accurate results than others (Mabsout, *et al.* 1997). One typical application of finite element analysis is to determine live load distribution factors in highway bridges. The lateral distribution factor is an important parameter in highway bridge design. Using a distribution factor, the lateral effect of live load on a bridge beam is simply decoupled from the longitudinal effect. As a result, bridge engineers can conveniently determine the maximum moment and shear of an individual beam in a bridge due to live load by multiplying the distribution factor to the maximum moment and shear obtained from a single beam analysis under truck load.

The American Association of State Highway and Transportation Officials Load Resistance and Factor Design (AASHTO LRFD) Specifications (AASHTO 1994) presents a set of equations for calculation of live load distribution factors for both moment and shear. Most variables in these equations contain ranges of applicability. These variables include span length, beam spacing, slab

† Graduate Research Assistant
‡ Associate Professor

thickness, beam stiffness, and number of beams. When the variables are within their range of applicability, the distribution factors calculated from these equations are considered accurate. However, the equations become less accurate when the ranges of applicability are exceeded. The AASHTO LRFD Specifications state that a refined analysis should be pursued for the distribution factors of bridge beams when the requirements and/or ranges of applicability of the equations are not met. Two of the most popular refined methods include the grillage analysis and the finite element analysis. The maximum moment under truck loads is determined from the refined analysis and used in the calculation of distribution factors. The AASHTO LRFD Specifications state that consideration shall be given to aspect ratios of elements, positioning and number of nodes, and other features of topology that may affect the accuracy of the analytical solution.

The objectives of this study were to investigate four different modeling techniques that can be used in modeling prestressed concrete beam bridges and to compare and evaluate the four techniques. Two bridges, one prestressed I-beam bridge and one prestressed box-beam bridge, were used to evaluate each modeling technique. In addition to the modeling techniques, other issues that directly affect the accuracy of analytical models such as torsional constant, support conditions, and support diaphragms are briefly discussed in this paper. The live load applied to all models was an AASHTO LRFD HL93 live load truck as classified in the AASHTO LRFD Specifications.

2. Literature review

2.1. Finite element modeling

Barker and Puckett (1997) explain that the bending of a beam-slab system causes in-plane effects at a beam-slab cross section. This bending produces compression in the deck slab and tension in the beam when positive moments are present. The deck slab itself will exhibit in-plane and out-of-plane effects that can be modelled by one element, commonly called a shell element. A typical shell element has three or four nodes with six degrees of freedom per node. The beams in a bridge superstructure can typically be modeled with beam or frame elements. The beam/frame element is a two-node element with six degrees of freedom per node. The eccentricity of the beam (composite beam) can be modeled by placing the beam elements at the centroidal axis of the beam, which creates additional degrees of freedom. These additional degrees of freedom may be related to the degrees of freedom of the shell by assuming a rigid linkage exists between the two points. A few of the terms used by some programs for this rigid linkage are: rigid link, element offset, or element eccentricities. Another approach to link the beam and slab is to use the additional degrees of freedom at the beam level but to declare them as slaves to the deck nodes directly above.

Mabsout, *et al.* (1997) reported a comparative study of four finite element modeling techniques. These techniques were used to model steel beam highway bridges. Nonlinear behavior was not considered in this study. In the first model, the concrete slab was idealized as quadrilateral shell elements and the steel beams were idealized as space frame members. The centroid of each beam coincided with the centroid of the concrete slab. The second model idealized the concrete slab as quadrilateral shell elements and space frame members eccentrically connected to the shell elements. Rigid links were used to connect the space frame and shell elements at their centroids on beam lines. The third model idealized the concrete slab and steel beam web as quadrilateral shell elements and the beam flanges as space frame elements. The flange to deck eccentricity was modeled by

imposing a rigid link. The fourth model idealized the concrete slab by using isotopic eight node brick elements. Both the steel beam flanges and web were modeled using quadrilateral shell elements. It was concluded that when using the first model, sufficient accuracy could be obtained for typical steel bridges. The other cases could also be used, but require more input time. The uses of the other models also require the beam moment to be calculated from stress values at critical locations.

In a study conducted by Chen and Aswad (1996), the bridge beam-deck structural system was modeled using both shell and beam (stiffener) elements. A standard quadrilateral (four-node) shell element of constant thickness was used when modeling the horizontal slab. Prestressed I-beams were described using standard isoparametric beam elements. The composite action of the beam and slab was accomplished by connecting the center of the slab and beam with rigid links. Chen (1999) pointed out that box-shaped girders could also be represented by 2-node isoparametric beam elements.

2.2. Quality control check for finite element models

When utilizing the finite element method, it is essential to perform a check on the computer output to ensure the results are accurate. Chen and Aswad (1996) suggested comparing the average tensile stress, f_{avg}, in the bottom fiber computed from the finite element analysis with that predicted by the beam formula:

$$f_{avg} = \frac{N_L M_{cen}}{N_g(\text{average } S_{bc})} \tag{1}$$

where N_L = number of loaded lanes; M_{cen} = midspan moment per lane; N_g = number of beams; and S_{bc} = composite section modulus at bottom fiber of beam. Eq. (1) is equivalent to the total applied moment check:

$$\sum M_c = N_L M_{cen} \tag{2}$$

where $\sum M_c$ = summation of beam moments.

3. Finite element modeling

Four different modeling techniques were investigated in this study. The first three modeling techniques (cases 1-3) described herein were implemented using the commercial finite element analysis program ANSYS 6.1. SAP 2000 was used for modeling case 4. Typically, when considering distribution factor calculations, concrete cracking is not considered. Therefore, linearly elastic behavior was assumed in the study.

For cases 1-3, a BEAM44 element was chosen to idealize the prestressed beams in the bridge superstructure. This is a uniaxial element with tension, compression, torsion, and bending capabilities. The element has six degrees of freedom at each node. It allows a different unsymmetrical geometry at each end and permits the end nodes to be offset from the centroidal axis of the beam (ANSYS 2002). In all models, the beams were typically meshed as 305 mm long elements.

For modeling case 4, a frame element was used to idealize the composite section consisting of both the prestressed beam and slab. The frame element uses a general three-dimensional beam-column formulation, which includes the effects of biaxial bending, torsion, axial deformation, and

biaxial shear deformations (SAP 2002).

A SHELL63 element was chosen to idealize the deck slab for cases 1-3. This element has both bending and membrane capabilities. Both in-plane and normal loads are permitted. The element has six degrees of freedom at each node. Stress stiffening and large deflection capabilities are also included (ANSYS 2002). The typical sizes of shell elements for the deck slab in this study were 305 mm by 305 mm. For modeling case 4, shell elements were used in order to connect the composite beam sections. The elements were connected at the composite beam centroid. For skewed models, triangular shell elements were used near the support locations to accommodate the change in geometry and to allow for better load distribution.

3.1. Modeling techniques

Similar to the research conducted by Mabsout, *et al.* (1997), the first modeling technique, case 1, considers the beam and deck slab to share the same centroid as shown in Fig. 1(a). In the present study, the accuracy of this technique is investigated for precast/prestressed concrete beam bridges.

ANSYS has the capability of offsetting the beam element from a reference node. This capability was incorporated into case 2, shown in Fig. 1(b). The reference nodes lie in the same plane as the deck slab centroid. The offset is equal to the distance between the slab centroid and the beam centroid. The offset distance is specified with the beam element properties. Offsetting the nodes in this manner enables complete composite action between the beam and deck slab by applying a rigid linkage between the two points.

Case 3, shown in Fig. 1(c), considers the beam nodes to be coupled with the nodes in the slab directly above them. The nodes of the beam and corresponding slab are coupled such that the two nodes will have the same displacements. In this case, the beam and slab centroids are located in positions that replicate an actual bridge superstructure. The location of the beam and slab centroid is similar to case 2, the only difference being the nodes are physically offset in the model.

For modeling case 4, shown in Fig. 1(d), the actual composite section consisting of both beam and slab was used. The composite section was created in SAP's Section Designer. Creating the section in this manner allowed the transformation from one material to the other to be simplified. The program calculated the composite section properties based on the base material, which was defined as the deck slab material. By taking advantage of this process, the composite moment at a given section was easily read from the output without the need for stress values. This case was comparable to case 2, since composite action was being considered.

The corresponding bending stress distribution diagrams for cases 1 - 4 are shown in Fig. 2. The stress distribution for case 4 was calculated based on the moment on the composite section obtained from SAP output. The stress distribution shown in Fig. 2(a) and Fig. 2(c) show two separate elements acting as individual flexural members. The only difference between these two cases is the location of the deck slab within the analytical model. From Fig. 2(b) and Fig. 2(d), it can be observed that the stress distribution is that of a composite section.

3.2. Torsional constant

Consideration must be given to the St. Venant torsional constant, J, when utilizing the finite element method. The AASHTO LRFD Specifications state that in lieu of more refined information, the torsional constant may be determined by the following equations assuming that the concrete

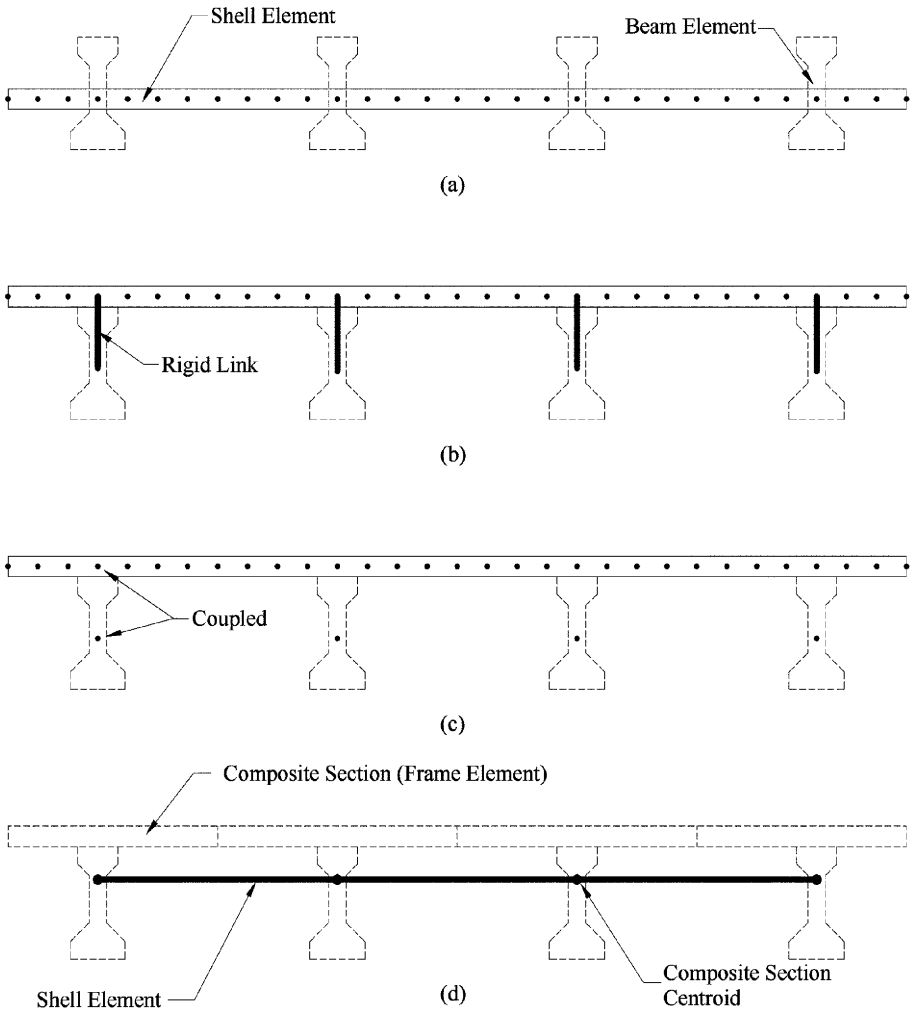

Fig. 1 Modeling techniques: (a) case 1- nodes coincide; (b) case 2 - beam offset; (c) case 3 - coupled nodes; and (d) case 4 - SAP section designer

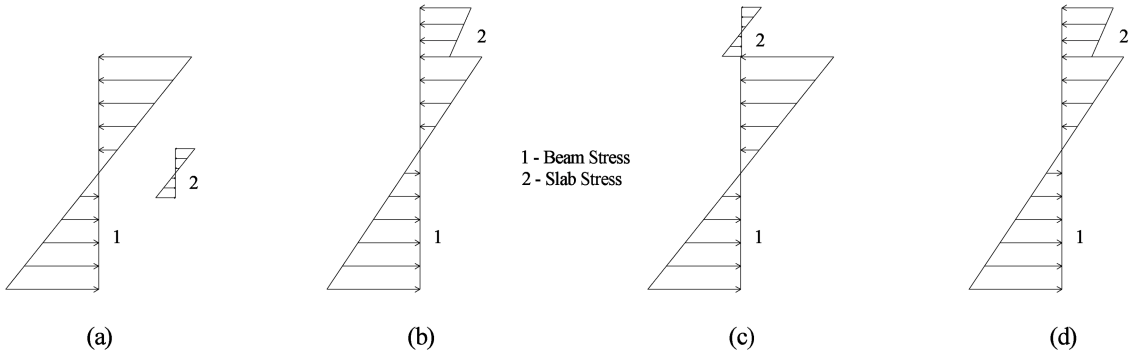

Fig. 2 Bending stress distribution diagrams: (a) case 1; (b) case 2; (c) case 3; and (d) case 4

sections remain linear, elastic, and uncracked.

For stocky open sections, e.g., prestressed I-beams, T-beams, etc., and solid sections:

$$J \approx \frac{A^4}{40.0 I_p} \tag{3}$$

For closed thin-walled shapes, e.g., steel and concrete box sections:

$$J \approx \frac{4A_o^2}{\sum (s/t)} \tag{4}$$

where b = width of plate element; t = thickness of plate-like element; A = area of cross section; I_p = polar moment of inertia; A_o = area enclosed by centerlines of elements; and s = length of a side element.

Another approximate method for calculating the torsional constant involves using idealized rectangular sections (Sanders and Elleby 1970). For a girder consisting of three idealized rectangles, the torsional constant can be calculated as follows:

$$J = \sum_{i=1}^{3} K_i w_i d_i^3 \tag{5}$$

where K_i is a coefficient that can be found in many books on elastic analysis; w_i = smaller side of rectangle; and d_i = longer side of rectangle.

3.3. Support conditions

Typically, the support conditions for a single span bridge consist of a hinge at one abutment and a roller at the other abutment. For a multi-span bridge, the same concept holds true when the longitudinal movement is not fully restrained. Usually, a hinge is used at one abutment, while a roller is placed at all interior supports and the other abutment. The hinge maintains the structural stability of the bridge, while the roller allows for expansion and contraction of the bridge. The support conditions for a real bridge may be specified as a hinge and roller, but it is possible for the supports to possess a certain amount of fixity. A roller support may not roll due to the presence of a diaphragm, friction at the joint, etc. In this study, two support conditions for each bridge were studied, one with hinges and rollers and the other with all hinges. The all-hinges condition is similar to the support condition that might be expected for an integral bridge. A hinge was modeled by restraining all three translational degrees of freedom, e.g., UX, UY, and UZ. A roller was modeled by restraining only the UY and UZ degrees of freedom, which allowed translation in only the global X direction, the longitudinal direction of the bridge. By comparing the hinge-roller supports to the all-hinged supports, the sensitivity of the support conditions can be assessed.

3.4. Presence of diaphragms

Many researchers have studied the effect of support diaphragms and intermediate diaphragms. Intermediate diaphragms have been shown to distribute load more evenly, however, their presence

has also been shown to make the girders more vulnerable to damages due to lateral impacts (Sengupta and Breen 1973). Because intermediate diaphragms were not used in the two bridges in this study, they were not considered in the bridge models. However, the effect of support diaphragms was investigated for both bridges. Typically, support diaphragms are considered to provide stability for the supporting beam members as well as continuity over interior support locations. In both bridges studied, the support diaphragms were made of reinforced concrete and, therefore, were modeled by using a beam/frame element.

3.5. Quality control checks for skewed bridge models

The purpose of a quality control check is to ensure that the FEA model for a bridge is developed correctly and the actual behavior of the bridge member is reflected accurately in the analysis results. As indicated in the previous section, Chen and Aswad (1996) suggested checking the total applied moment, $N_L M_{cen}$, with the summation of beam moments obtained from analysis, $\sum M_c$, as shown in Eq. (2). However, this equation is only valid for nonskewed bridges. When a skewed bridge model is analyzed, the summation of beam moments from the analysis becomes smaller than the total applied moment. This is because the load transfer paths in the bridge are much more complex when the support lines are skewed. For a skewed bridge model, instead of the total applied load being transferred to supporting beams as expected, part of the applied load is transferred directly to the nearest support through the deck slab. The load transfer path is dependent on the angle of skew, the stiffness ratio of transverse member (deck slab) to longitudinal member (beam), the spacing of beams, and the length of the bridge. In order to consider the reduction of beam moments due to the skewness of a bridge, a simple reduction factor equation for the quality control check, Eq. (6), was developed through this study. Using the reduction factor from Eq. (6), a definite moment that is carried by all beams in a skewed bridge can be determined by multiplying the reduction factor to the total moment based on a beam line analysis and the number of trucks applied. The equation for model quality control check is expressed in Eq. (7). If a finite element analysis model is correctly developed for a bridge, the definite moment should be approximately equal to the summation of total beam moments.

$$F_{skew} = 1.0 - \left(\frac{S}{L}\right)^{\alpha}\left(\frac{t_s}{d}\right)^{\beta}(\tan\theta)^{1.5} \tag{6}$$

$$\sum M_c = F_{skew} N_L M_{cen} \tag{7}$$

where F_{skew} = skew reduction factor for quality control check; S = spacing of beams (m); L = span length (m); t_s = thickness of slab (mm); d = depth of beam (mm); θ = skew angle (deg.); $\sum M_c$ = summation of beam moments; N_L = number of loaded lanes; and M_{cen} = midspan moment per lane from two-dimensional analysis. The term $F_{skew} N_L M_{cen}$ is the definite moment. The variables α and β are dependent on bridge type. For the prestressed concrete I-beam bridge, the variables α and β are –0.2 and 2.0, respectively. For the prestressed concrete spread box beam bridge, the variables are 0.1 and 1.3, respectively.

4. Application of modeling techniques to two bridges

Two prestressed concrete slab-on-beam bridges were used for application and evaluation of the four modeling techniques. Finite element models were generated to determine the maximum moments in the interior and exterior beams. Multiple trucks were positioned on each bridge and moved in both the longitudinal and transverse direction in order to obtain the maximum moment. Only one truck could occupy a lane at a time in the longitudinal direction (AASHTO 1994, 1996), but the number of trucks in the transverse direction depended on the roadway width. Due to the application of multiple presence factors, two trucks traveling in the same direction resulted in the maximum moment for both interior and exterior beams.

4.1. Two-span continuous prestressed concrete I-beam bridge

The two-span bridge herein was modified from the Pistol Creek Bridge located in Blount County, Tennessee. Pistol Creek Bridge has five spans of approximately 22900 mm each. For the convenience of modeling and analysis, only two of the five spans were used and slight modifications were made to the bridge geometry. The two-span bridge has a total length of 45800 mm, 22900 mm for each span. The thickness of deck slab is 216 mm and it is supported by five lines of AASHTO Type III prestressed beams. The specified compressive strengths of concrete for beam and slab are 41MPa and 28MPa, respectively. The actual bridge is a non-skewed bridge. To observe how the live load moment changes in a skewed bridge, a second model was analyzed with a skew angle of 45°. The skew angle was measured from a line perpendicular to the beam lines to the support lines of the bridge. The plan view of each bridge model and the typical cross section of the bridge are shown in Fig. 3. The finite element mesh of the non-skewed bridge model is shown in Fig. 4.

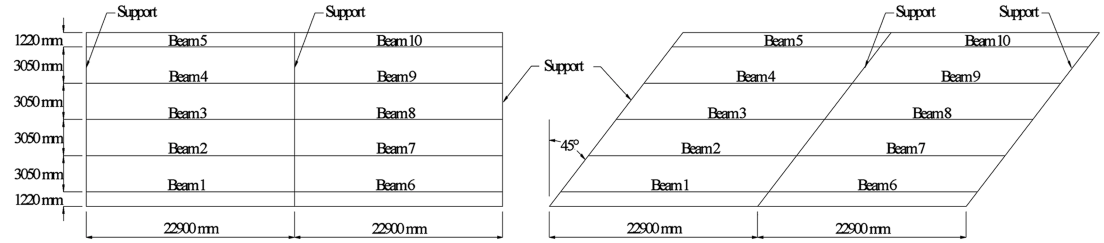

(a)

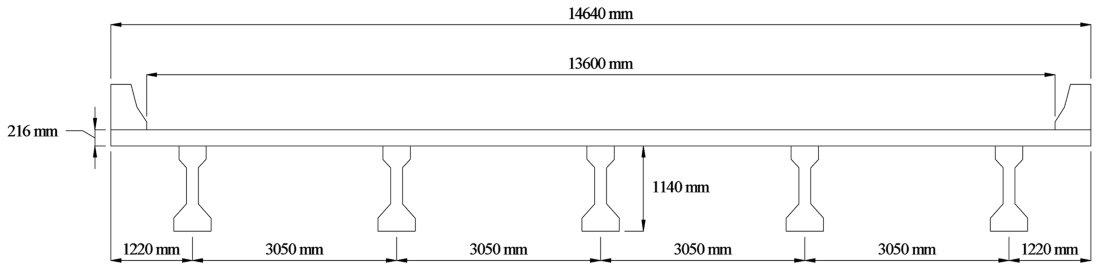

(b)

Fig. 3 Two-span prestressed I-beam bridge: (a) plan view and (b) typical cross section

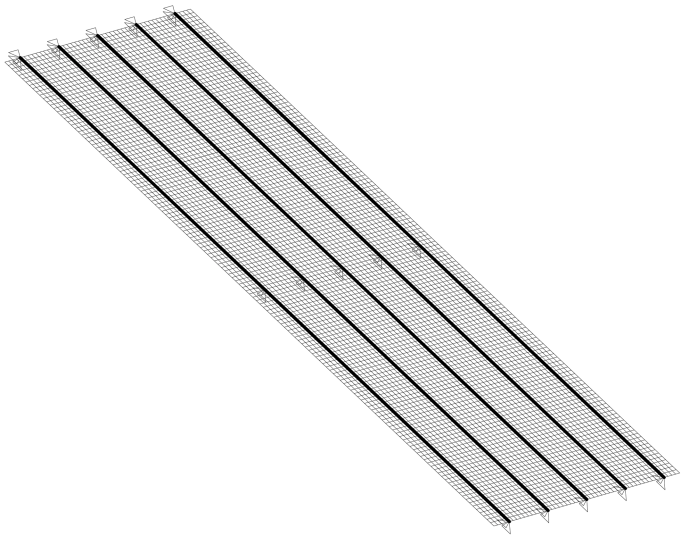

Fig. 4 Typical finite element mesh and support restraints

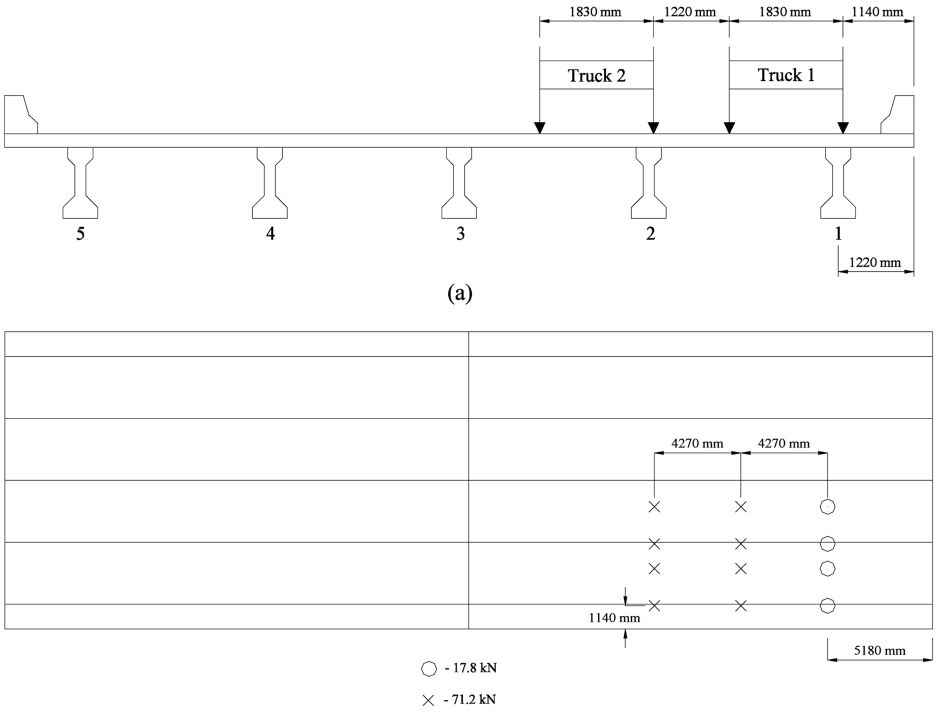

Fig. 5 Loading position for non-skewed bridge (prestressed I-beam bridge): (a) transverse location and (b) longitudinal location

Table 1 Beam moments for non-skewed bridge (prestressed I-beam bridge)

Beam	Moment (kN-m)							
	0^o Skew angle				45^o Skew angle			
	case				case			
	1	2	3	4	1	2	3	4
1	899	894	932	876	839	819	875	836
2	800	903	820	912	734	840	751	834
3	462	451	463	448	427	440	430	415
4	173	86	156	98	178	104	174	105
5	21	26	30	25	41	12	36	27
Total	2355	2361	2400	2359	2218	2215	2265	2217
Difference	0.40%	0.64%	2.34%	0.59%	0.17%	0.05%	2.29%	0.13%

The moments from finite element analysis are shown in Table 1 and are based on the loading position shown in Fig. 5. The trucks were positioned so that the maximum moment in an exterior and an interior beam could be obtained. Similar trends were observed in the moments changes for all modeling cases when the skew angle was increased to 45°. With the increase in skew angle, the moments in the interior and exterior beam were reduced.

The quality control check was performed by running a beam line analysis, which involved the analysis of one beam loaded with one truck. The resulting maximum moment for this case was 1173 kN-m. The percent differences shown in Table 1 were calculated as follows:

$$\% \text{ Difference } = \frac{(\sum \text{moment from } FEA) - (F_{skew} N_L M_{cen})}{(F_{skew} N_L M_{cen})} \tag{8}$$

As shown in Table 1, for the model with no skew, the summation of the moments for each case is approximately 2346 kN-m. The differences are well below +/- 1%. When comparing the average bottom fiber stresses for case 2, the difference between Eq. (1) and finite element results is approximately 2.3%. For the model with a 45° skew angle Eqs. (6) and (7) were used before calculating the percent difference. From Eq. (6), $F_{skew} = 0.944$ resulting in a definite moment of 2214 kN-m. Using the definite moment, the percent differences for all but case 3 are well below 1.0%. One point worth noting is the difference in the distribution of moment to each supporting member when different modeling cases are used. With reference to Table 1, cases 1 and 3 resulted in a moment distribution that was gradually spread out from the heavily loaded beams to other supporting members. For cases 2 and 4, beams 1, 2, and 3 are shown to carry the majority of the load. Because the beams and slab were acting compositely, the stiffness of the section is increased as compared to the other cases and therefore, more load is carried by these members. As a result, the load distribution was relatively localized, so members that were closer to the applied load resisted most of the load. Since cases 2 and 4 model the composite action between the beam and slab, the live load distribution from these two modeling cases should better represent the true behavior of the actual bridge.

The same models were also analyzed with different support conditions, hinge-roller supports and

Table 2 Moments with support diaphragms present (prestressed I-beam bridge)

Beam		Moment (kN-m)			
		Exterior		interior	
Skew angle (deg)		0	45	0	45
case	1	869	802	784	702
	2	898	847	898	816
	3	932	852	820	734
	4	867	819	901	822
Max. diff. between *w*/and *w*/*o* support diaphragms		-3.32%	-4.44%	-1.98%	-4.38%

all hinged supports. Support diaphragms were not included in these models. Only cases 1 and 2 were investigated because they yield similar results to cases 3 and 4, respectively. Changing the support conditions did not affect the results for case 1. However, the beam moments for case 2 were slightly different when different support conditions were applied. In general, the beam moments with all hinged supports were lower than those with hinge-roller supports. The only exception was the exterior beam for the 45° skew model. The all hinged condition resulted in an increase in moment by approxmately 4.9%. The maximum difference for the interior beam for both skew angles considered was only −1.5%.

For each modeling technique, the effect of support diaphragms was investigated. Diaphragms were placed between beams over pier and abutments across the bridge width. The results for each model with diaphragms are shown in Table 2. The presence of diaphragms at the supports resulted in a reduction in the live load moment for both interior and exterior beams. For each skew angle considered, the maximum reduction for the exterior and interior beam was 4.44% and 4.38%, respectively.

4.2. Simply-supported prestressed concrete spread box-beam bridge

The simply supported prestressed box-beam bridge was modified from the Del Rio Pike Bridge, located in Williamson County, Tennessee. This one span bridge of approximately 21340 mm crosses

Table 3 Beam moments for skewed bridge (prestressed box-beam bridge)

Beam	Moment (kN-m)							
	0^o Skew angle				45^o Skew angle			
	case				case			
	1	2	3	4	1	2	3	4
1	587	637	684	595	443	564	620	508
2	580	628	640	607	429	533	568	508
3	547	572	560	576	392	475	495	472
4	502	474	455	465	343	390	393	368
5	455	365	330	387	306	295	322	292
Total	2671	2677	2669	2631	1913	2257	2398	2148
Difference	0.49%	0.73%	0.44%	-1.01%	-13.59%	1.95%	8.31%	-2.98%

the West Harpeth River and is supported by five prestressed concrete spread box beams. The thickness of the deck slab is 210 mm. The specified compressive strength of concrete is 38 MPa for beam and 28 MPa for deck slab. The actual bridge has a skew angle of approximately 49°, but for the convenience of modeling, a skew angle of 45° was used. For the purpose of comparison, this bridge was also modeled with no skew angle to observe the effect of skew. Fig. 6 shows the plan view of both bridge models and the typical cross section. Both models, with skew and without skew, were also analyzed to investigate the impact of different support conditions and the presence of support diaphragms.

The moment values from finite element analysis are listed in Table 3. The beam moments in Table 3 demonstrate the load distribution pattern across the bridge for each modeling case. It can be seen from Table 3 that case 3 moment values for the 0° skew model are higher than both cases 2 and 4 for the beams near the loading location. For the 45° skew model, case 3 moment values are higher than all other cases for all beams. Since composite action between the beams and slab is being modeled for cases 2 and 4, thereby giving a better representation of the actual response of the bridge members, the observation of case 3 results suggest a certain degree of inaccuracy with this modeling case.

The moment values shown in Table 3 were also used in the quality control check for each modeling case. The maximum moment from the beam line analysis was M_{cen} = 1329 kN-m and the number of loaded lanes was N_L = 2. Using Eq. (8), the percent differences for both models were calculated. For the model with no skew, the differences were well below 1% for cases 1-3, and only

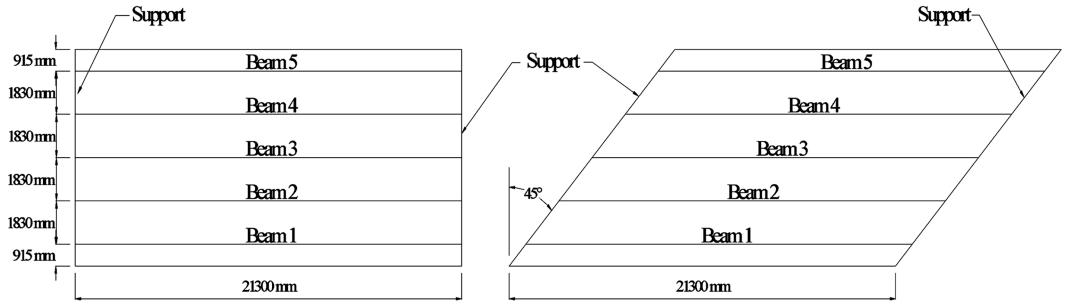

(a)

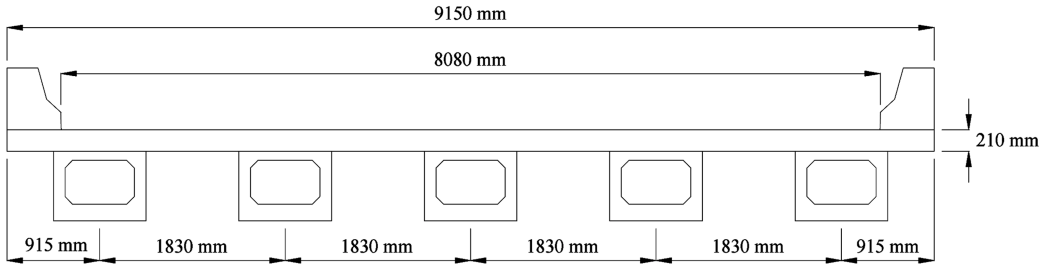

(b)

Fig. 6 Single-span prestressed box-beam bridge: (a) plan view and (b) typical cross section

Table 4 Comparison of models with and without support diaphragms (prestressed box-beam bridge)

Beam	Moment (kN-m)							
	Exterior				Interior			
Case	1	2	3	4	1	2	3	4
with Diaphragm	443	564	620	508	429	533	568	508
without Diaphragm	418	534	610	479	404	515	561	487
Difference	-5.61%	-5.27%	-1.69%	-5.76%	-5.85%	-3.36%	-1.26%	-4.00%

2% for case 4. The difference between Eq. (1) and finite element results for case 2 is approximately 0.8%. For the 45° skew model, the skew reduction factor, $F_{skew} = 0.833$ by using Eq. (6). The definite moment for the quality control check was calculated using Eq. (7) and was equal to 2214 kN-m. As shown in Table 3, the difference between the definite moment and the summation of beam moments for cases 2 and 4 was reasonablely small. However, a larger discrepancy was oberved for cases 1 and 3. The reason for this large difference could be related to many factors such as no composite action between the beams and slab and/or the relatively smaller stiffness ratio of prestressed beam and cast-in-place concrete deck slab. Due to these factors more load effect was directly transferred to the bridge supports through the slab.

Each model was analyzed with the hinge-roller and all-hinged support conditions. The beam moments with all-hinged supports were lower than those with hinge-roller supports. A maximum decrease of about 5.5% was observed for both the exterior and interior beams for the model with no skew.

Diaphragms were placed at both end support lines in order to investigate their effect on live load distribution. The diaphragms were modeled noncompositely with the deck slab. A hinge-roller support condition was used for this model. The results for the model with a 45° skew angle are shown in Table 4. It can be observed from Table 4 that the support diaphragms have a small effect on the moment magnitude. The moment values were reduced by a maximum of 5.61% and 5.85% for the exterior and interior beam, respectively.

A sensitivity analysis was performed on this bridge in order to determine the change in moment results when the element size was increased. The non-skewed model was used for the analysis and only case 2 was investigated. The same transverse and longitudinal loading location was used with the model of large size of elements as was used with the finer meshed model. The use of the larger element sizes (610 mm x 610 mm) resulted in a total moment difference of 1.4% to the exact value, while the difference for the finer mesh (305 mm x 305 mm) was only 0.7%. When comparing the average bottom fiber stress with Eq. (1), a larger difference was observed from the model with larger size of elements. Based on this analysis the finer mesh models used in the study should yield more accurate results.

5. Model verification through field testing

The validation of a finite element model is typically done by use of experimental results. Shahawy and Huang (2001) showed a comparison between theoretical and experimental results for seven concrete slab-on-girder bridges. The finite element model used in the study was similar to the case 2 model discussed in this paper. The bridge deck between girders was modeled as a series of quadrilateral plate and shell elements with six degrees of freedom at each node. The girders were

modeled using space bar elements. A rigid link was used to connect the centroid of the beam to the centroid of the slab. The test results were found to be very close to those obtained by the finite element model indicating the accuracy of the modeling technique.

The modeling and analysis techniques presented by Chen (1995, 1999) and Barr, *et al.* (2001), similar to case 2, were verified by comparing the finite element results to experimental results. Excellent agreement was shown between the analytical model and field measurements.

6. Conclusions

Finite element analysis can be used effectively to determine the maximum responses, such as moment and shear, in bridge beams when the bridge is modeled and analyzed properly. With the maximum response values obtained, distribution factors can be easily calculated. The AASHTO LRFD Specifications demand refined analysis such as finite element analysis when the ranges of applicability of the variables in the distribution factor equations are exceeded. Selecting the correct modeling technique is very important to accurately perform a rigorous analysis method, such as finite element analysis. In this paper, a prestressed I-beam bridge and a prestressed spread box-beam bridge were modeled using four modeling techniques. The feasibility and correctness of each modeling technique were examined. The following can be concluded from this study:

- Modeling cases 1, 2, and 4 can be used to effectively and efficiently model the bridge superstructures presented in this paper. Composite action between prestressed beam and cast-in-place deck has an impact on the magnitude and distribution pattern of beam moments in a bridge. Upon further comparison of cases 1, 2, and 4, it was found that cases 2 and 4 better represent the behavior of actual slab-on-beam bridges because of the inclusion of composite action. The literature review revealed that the accuracy of modeling case 2 has been verified by use of experimental results. The applicability of these modeling techniques to other bridge types should be investigated before utilization.
- The distribution of truck loads were more localized for the composite modeling cases (cases 2 and 4) and more evenly distributed for the noncomposite modeling cases (cases 1 and 3).
- A proper quality control check is necessary to ensure the correctness of the modeling technique. The equations for a quality control check for a non-skewed bridge were presented in the literature review. The equations for a skewed bridge were developed and presented in this paper.
- Special consideration must be given to the calculation of the St. Venant torsional constant. The torsional constant should be calculated by using the most accurate methods available. When the concrete sections are assumed to remain linear, Eq. (3) through Eq. (5) give a good approximation for the applicable sections.
- The finite element analysis results were shown to be sensitive to the changes in support condition. The supports should be modeled according to the actual bridge situation. It is therefore recommended that engineers use their own judgment when modeling support conditions.
- The presence of support diaphragms had a minor impact in the load distribution for both bridges investigated. The reduction in the moment values due to presence of a diaphragm was less than 7% for all cases considered.

Acknowledgements

The authors would like to acknowledge the financial support provided by Tennessee Technological University for this study. The content of this paper reflect the views of the authors and do not necessarily represent the views of the sponsors.

References

Abendroth, R. E., Klaiber, R. W. and Shafer, M. W. (1995), "Diaphragm effectiveness in prestressed-concrete beam bridges", *J. Bridge Eng.*, **121**(9), 1362-1369.

American Association of State Highway and Transportation Officials (AASHTO) (1994), *AASHTO LRFD Bridge Design Specifications*, 1st Ed. Washington, D.C.

American Association of State Highway and Transportation Officials (AASHTO) (1996), *Standard Specifications for Highway Bridges*, 16th Ed. Washington, D.C.

ANSYS documentation version 6.1 (2002), ANSYS Inc.

Barker, R. M. and Puckett, J. A. (1997), *Design of Highway Bridges: based on AASHTO LRFD bridge design specification*, John Wiley, New York.

Barr, P. J., Eberhard, M. O., and Stanton, J. F. (2001), "Live-load distribution factors in prestressed concrete girder bridges", *J. Bridge Eng.*, **6**(5), 298-306.

Chen, Y. (1995), "Refined and simplified methods of lateral load distribution for bridges with unequally spaced girders: I. Theory", *Comput. Struct.*, **55**(1) 1-15.

Chen, Y. (1999), "Distribution of vehicular loads on bridge girders by the FEA using ADINA: modeling, simulation, and comparison", *Comput. Struct.*, **72**(1-3), 127-139.

Chen, Y. and Aswad, A. (1996), "Stretching span capability of prestressed concrete bridges under AASHTO LRFD", *J. Bridge Eng.*, **1**(3), 112-120.

Eom, J. and Nowak, A. S. (2001), "Live-load distribution for steel beam bridges", *J. Bridge Eng.*, **6**(6), 489-497.

Mabsout, M. E., Tarhini, K. M., Frederick, G. R. and Tayar, C. (1997), "Finite-element analysis of steel beam highway bridge", *J. Bridge Eng.*, **2**(3), 83-87.

Sanders, W. W. Jr, and Elleby, H. A. (1970), "Distribution of wheel loads on highway bridges", National Cooperative Highway Research Program Report No. 83, Transportation Research Board, Washington, D.C.

SAP 2000 Analysis Reference Manual (2002), Computers and Structures, Inc.

Sengupta, A. and Breen, J. E. (1973), "The effect of diaphragms in prestressed concrete girder and slab bridges", Res. Report 158-1F, Project 3-5-71-158, Center for Highway Res. Univ. of Texas at Austin, TX.

Shahawy, M. and Huang, D. (2001) "Analytical and field investigation of lateral load distribution in concrete slab-on-girder bridges", *ACI Struct. J.*, **98**(4), 590-599.

CM